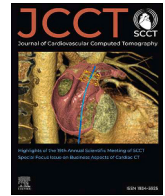




Contents lists available at ScienceDirect

## Journal of Cardiovascular Computed Tomography

journal homepage: [www.JournalofCardiovascularCT.com](http://www.JournalofCardiovascularCT.com)

## Research Paper

# Diagnostic accuracy of energy-integrating and standard-resolution photon counting detector CT for coronary artery stenosis grading in CCTA: A comparative study

Susann Skoog<sup>a,b,\*</sup>, Christos Pagonis<sup>c</sup>, Mårten Sandstedt<sup>a,b</sup>, Lilian Henriksson<sup>a,b</sup>,  
Håkan Gustafsson<sup>b,d</sup>, Anders Persson<sup>a,b</sup>, Erik Tesselaar<sup>b,d</sup>

<sup>a</sup> Department of Radiology and Department of Health, Medicine and Caring Sciences, Linköping University, Linköping, Sweden

<sup>b</sup> Center for Medical Image Science and Visualization (CMIV), Linköping University, Linköping, Sweden

<sup>c</sup> Department of Cardiology, Department of Health, Medicine and Caring Sciences, Linköping University, Linköping, Sweden

<sup>d</sup> Department of Medical Radiation Physics, Department of Health, Medicine and Caring Sciences, Linköping University, Linköping, Sweden

## ARTICLE INFO

## Keywords:

PCD-CT

CCTA

CAD

Stenosis assessment

Image quality

## ABSTRACT

**Background:** Coronary CT angiography (CCTA) is a key non-invasive tool for evaluating coronary artery disease (CAD). While energy-integrating detector CT (EID-CT) offers high negative predictive value (NPV), its positive predictive value (PPV) is limited in heavily calcified vessels. Photon-counting detector CT (PCD-CT), with higher spatial resolution and reduced blooming, may enhance diagnostic performance. Current PCD-CT systems provide both standard-resolution (SR) and ultra-high-resolution (UHR) modes, but the clinical impact of these modes remains under investigation.

**Objectives:** To compare the diagnostic accuracy and image quality of SR-PCD-CT versus EID-CT in quantifying coronary stenosis, using quantitative coronary angiography (QCA) as reference.

**Materials and methods:** In this prospective, single-centre study, 21 patients (5 women, mean age 71.5 years) with suspected CAD underwent CCTA with both EID-CT and SR-PCD-CT prior to QCA. A total of 301 coronary segments were assessed for stenosis severity, with  $\geq 50$  % stenosis deemed significant. Image quality was graded using a 5-point scale.

**Results:** No significant differences in percentage diameter stenosis (%DS) were found between imaging techniques ( $p = 0.20$ ). Both EID-CT and SR-PCD-CT showed good agreement with QCA (AUC: PCD-CT 0.89, EID-CT 0.86). Specificity and NPV were high for both; sensitivity and PPV were moderate. SR-PCD-CT yielded higher image quality compared to EID-CT ( $p < 0.001$ ).

**Conclusions:** In standard resolution mode, PCD-CT offers excellent image quality for quantifying coronary stenosis at comparable diagnostic accuracy compared to EID-CT.

## 1. Introduction

Coronary artery disease (CAD) occurs when atherosclerotic plaque forms in the coronary artery walls, restricting blood flow to the myocardium, leading to myocardial ischemia.<sup>1</sup> While historically, CCTA has primarily been used to rule out CAD in patients with low to intermediate cardiovascular risk, recent guidelines from the European Society of Cardiology recommend CCTA as the first-line non-invasive imaging test for individuals with a 5–50 % pre-test likelihood of obstructive CAD.<sup>2</sup>

Conventional energy-integrating detector computed tomography (EID-CT) is limited by spatial resolution and calcium blooming artifacts, which can lead to overestimation of luminal stenosis, particularly in the presence of heavily calcified plaques. Large calcifications may obscure adjacent smaller lesions, further complicating accurate stenosis assessment.<sup>3</sup> These limitations may reduce the accuracy of stenosis assessment and contribute to the modest positive predictive value (PPV) reported for CCTA compared with invasive reference standards. Consequently, stenosis grading in clinical practice is commonly performed using

\* Corresponding author. Department of Radiology, Linköping University Hospital, 581 85 Linköping, Sweden.

E-mail addresses: [Susann.Skoog@liu.se](mailto:Susann.Skoog@liu.se), [Susann.Skoog@regionostergotland.se](mailto:Susann.Skoog@regionostergotland.se) (S. Skoog), [Christos.Pagonis@regionostergotland.se](mailto:Christos.Pagonis@regionostergotland.se) (C. Pagonis), [Marten.Sandstedt@regionostergotland.se](mailto:Marten.Sandstedt@regionostergotland.se) (M. Sandstedt), [Lilian.Henriksson@regionostergotland.se](mailto:Lilian.Henriksson@regionostergotland.se) (L. Henriksson), [hakan.l.gustafsson@liu.se](mailto:hakan.l.gustafsson@liu.se) (H. Gustafsson), [anders.persson@liu.se](mailto:anders.persson@liu.se) (A. Persson), [Erik.Tesselaar@liu.se](mailto:Erik.Tesselaar@liu.se) (E. Tesselaar).

<https://doi.org/10.1016/j.jcct.2026.01.003>

Received 27 October 2025; Received in revised form 6 January 2026; Accepted 16 January 2026

Available online xxx

1934-5925/© 2026 The Authors. Published by Elsevier Inc. on behalf of Society of Cardiovascular Computed Tomography. This is an open access article under the CC BY license (<http://creativecommons.org/licenses/by/4.0/>).

standardized semi-quantitative visual assessment frameworks, such as those recommended by the Society of Cardiovascular Computed Tomography and CAD-RADS<sup>4-6</sup>.

The latest advancement in CT is photon-counting detector CT (PCD-CT), which uses a detector design based on a single semiconductor layer to directly convert X-ray photons into electric signals, unlike conventional detectors that use indirect conversion.<sup>7</sup> This direct conversion allows for detectors with smaller detector elements, resulting in better visibility of small coronary vessels and less blooming of calcified plaques.<sup>8,9</sup> One of the clinically available PCD-CT systems supports both standard-resolution (SR) mode, which employs  $2 \times 2$  binning of detector elements, and ultra-high-resolution (UHR) mode, where individual detector elements are read out. While both modes provide higher spatial resolution than state-of-the-art EID-CT, the improvement in SR mode is relatively modest compared to UHR.<sup>10</sup> Previous studies have demonstrated that UHR acquisitions with thin slices (0.2 mm), sharp reconstruction kernels (e.g., Bv56/64), and retrospective helical gating can enhance edge sharpness and diagnostic accuracy<sup>11-13</sup>. On the other hand, SR mode provides a more robust acquisition, as it uses a larger detector width. This results in a shorter scan duration and less motion and stairstep artifacts, which is why SR mode often is the preferred scan mode in patients with low calcium scores or highly irregular heart rates, avoiding repeated acquisitions.

Invasive coronary angiography (ICA) with quantitative evaluations (QCA) of the percentage diameter stenosis remains the gold standard for evaluating the degree of stenosis in coronary vessels, often complemented by techniques like intravascular ultrasound, optical coherence tomography and measurement of fractional flow reserve (FFR). However, ICA has several drawbacks, including relatively high costs, limited availability, invasiveness, and potential serious complications.<sup>14,15</sup>

The primary aim of this study was to assess the degree of coronary artery stenosis using SR-PCD-CT and EID-CT, and to compare it with QCA. Additionally, the study evaluated and compared image quality between the two CT modalities. We hypothesized that the improved

spatial resolution of SR-PCD-CT, compared to EID-CT, would result in a higher PPV for detecting coronary stenosis.

## 2. Material and methods

### 2.1. Design and participants

The study was approved by the Swedish Ethical Review Authority (Dnr 2022-04666-01) and performed in accordance with the Declaration of Helsinki. Written informed consent was obtained from all study participants.

Participants in this open, prospective, observational study were enrolled between October 2022 and October 2024. Eligible participants were identified during referral for ICA due to suspected significant coronary stenosis on routine EID-CT CCTA. After inclusion, they underwent an additional CCTA with PCD-CT before ICA.

Inclusion criteria were suspected chronic coronary syndrome; typical stable angina classified according to the Canadian Cardiovascular Society (CCS) system (classes I-IV) with symptoms persisting for at least three months<sup>16,17</sup>; an intermediate pre-test probability of obstructive CAD based on the 2019 ESC recommendations<sup>18,19</sup>; and possible, suspected, or definite significant coronary stenosis on the initial CCTA.

Exclusion criteria were prior percutaneous coronary intervention (PCI), coronary artery bypass grafting (CABG) or known coronary anomalies; prior valve surgery; severely reduced kidney function (eGFR <35 ml/min); metallic implants in the chest or spine likely to impair image quality; acute coronary syndromes requiring urgent intervention; any supraventricular or ventricular arrhythmia; or known allergy to iodinated contrast agents.

### 2.2. CT image acquisition and reconstruction

#### 2.2.1. Patient preparation

Intravenous beta-blockers (Metoprolol 1 mg/mL), up to 10 mg, were administered to patients with a heart rate >60 bpm and a systolic blood

**Table 1**  
CT acquisition and reconstruction parameters for CCTA scans in EID-CT and PCD-CT.

Category	Parameter	EID-CT	PCD-CT
Scan technique	Scanner platform	SOMATOM Force (n = 6), SOMATOM Definition Flash (n = 12), SOMATOM Definition Edge (n = 3)	NAEOTOM Alpha
	Scan mode <sup>a</sup>	Flash, spiral	Flash, sequence, spiral
	Tube potential (kV) <sup>b</sup>	70, 80, 90, 100, 110, 120	140
	Quality reference (Qref, mAs)	250	–
	IQ level	–	64
	Spiral pitch	0.2–0.3	–
	Flash pitch	3.2	3.2
	Collimation (mm)	192 × 0.6	144 × 0.4
	Rotation time (s)	0.25	0.25
	Image reconstruction	Monoenergetic level (keV)	–
Reconstruction algorithm		ADMIRE4	QIR4
Reconstruction kernel		Bv36, Bv38	Bv44, Bv56, Bv64
Slice thickness (mm)		0.5	0.4
Slice increment (mm)		0.25 (n = 18), 0.3 (n = 3)	0.2
Field of view (mm)		135–188	135–188
Image matrix size		512	512 (n = 19), 1024 (n = 2)
Contrast protocol	Iodine dose (mgI/kg)	70 kV: 163 80 kV: 244 90–120 kV: 325	spiral/Flash: 244 sequence: 244
	Injection time (s)	11.5 (all levels)	11.5 (spiral/Flash), 13 (seq.)
	Contrast/saline mix	70 kV: 50/50 80 kV: 75/25 90–120 kV: 100/0	75/25 (all protocols)
	Total contrast dose (gI)	23.2 ± 6.1	20.4 ± 4.2
	Total DLP (mGy·cm)	450 ± 282	221.9 ± 150
Radiation dose	CTDI <sub>vol</sub> (mGy)	28.6 ± 18.7	14.7 ± 10.4

<sup>a</sup> Scan mode selection depends on patient size, heart rate, and heart rate variability.

<sup>b</sup> Tube potential in EID-CT was automatically adjusted based on patient size.

pressure >110 mmHg before the examination, unless contraindications were present. Additionally, nitroglycerine (glyceryl trinitrate 0.4 mg/dose sublingual spray) was administered at least 4 min prior to CCTA, with two doses given if blood pressure was >110 mmHg, and one dose if blood pressure was >100 mmHg. Examinations were performed using an injection protocol, with 50–100 % contrast agent (Omnipaque 350 mgI/mL) and 50–0 % saline (NaCl), depending on the tube voltage used. This was followed by a 70 mL saline chaser. The contrast dose was 244 mgI/kg in PCD-CT and 163–325 mgI/kg (depending on tube voltage) in EID-CT, up to a maximum weight of 77 kg (see Table 1). Before the diagnostic acquisition, a test bolus acquisition was performed, to determine the optimal bolus timing.

### 2.2.2. EID-CT

Patients underwent CCTA with EID-CT using any of three different scanners belonging to the same radiological department (SOMATOM Force, SOMATOM Definition Flash and SOMATOM Definition Edge, Siemens Healthineers, Forchheim, Germany). A standardized protocol was used, including a non-contrast scan for calcium scoring, followed by a contrast-enhanced, ECG-gated scan at a tube voltage between 70 and 120 kV, as determined by the dose modulation algorithm. Patients were scanned using prospective ECG-triggering with a prospectively gated high-pitch-spiral (Flash) protocol ( $n = 1$ ) or a retrospectively ( $n = 20$ ) gated acquisition, depending on the accessible scan modes and the patient's habitus, heart rate and heart rate variability. Images were reconstructed using a vascular kernel (Bv36,  $n = 6$  or Bv38,  $n = 15$ ). The reconstructed slice thickness was 0.5 mm, and the increment was 0.25 mm ( $n = 18$ ) or 0.3 mm ( $n = 3$ ), see Table 1.

### 2.2.3. PCD-CT

PCD-CT was performed using a dual-source PCD-CT system (NAEOTOM Alpha, Siemens Healthineers GmbH, Forchheim, Germany) using a standardized protocol. This protocol included a non-contrast scan for calcium scoring followed by a contrast-enhanced ECG-gated acquisition mode at a tube voltage of 140 kV. The contrast-enhanced scan was performed using a prospectively gated high-pitch spiral ( $n = 2$ ), sequential ( $n = 18$ ) scan mode or using a retrospectively gated spiral ( $n = 1$ ) acquisition, depending on the patient's heart rate and heart rate variability. Images were reconstructed using a vascular kernel (Bv44). Additional kernels (Bv56 and Bv64) were also available, except in three cases due to data loss. The smallest possible reconstructed slice thickness of 0.4 mm was used with an increment of 0.2 mm (Table 1).

### 2.3. Invasive coronary angiography (ICA)

ICA was performed according to clinical routine, with both visual assessment and/or QCA and, as indicated, invasive pressure indices during rest and with adenosine if needed. Depending on the localization and severity of the coronary lesions, treatment with either percutaneous coronary intervention (PCI) or coronary artery bypass grafting (CABG), or alternatively optimal medical therapy, was determined by the treating physicians in accordance with standard clinical practice.

### 2.4. CT quantitative stenosis assessment and image quality evaluation

CT images were analyzed using semi-automatic coronary analysis software (Coronary Analysis, syngo.Via VB60, Siemens Healthineers, Forchheim, Germany). Stenosis severity at the narrowest section of each segment of the coronary tree was quantified as diameter stenosis (%DS), defined as  $\%DS = [(reference\ lumen\ diameter - minimum\ lumen\ diameter)/reference\ lumen\ diameter] \times 100\ %$ . The reference lumen diameter was defined as the diameter of the nearest anatomically normal segment proximal (or, when appropriate, distal) to the stenosis. Plaque composition was assessed visually using conventional CCTA attenuation characteristics, classifying plaques as calcified, non-calcified, or mixed based on the relative proportion of high-

attenuation calcified components and low-attenuation non-calcified components.

Curved multiplanar reconstructions were used in the evaluation, using the sharpest available reconstruction kernel, as in clinical practice. All measurements were performed by a thoracic radiologist (S.S.) with 10 years of experience in cardiac CT interpretation. The reader independently evaluated the CCTA examinations from both EID-CT and PCD-CT, with a minimum interval of one week between assessments, and was blinded to the results from the other CT modality as well as to the ICA findings to minimize recall bias. In addition, key images were reviewed by a second radiologist (M.S.) with more than 10 years of experience in cardiac imaging. In cases of disagreement between the two readers, a consensus discussion was held, and manual corrections of the percentage diameter stenosis (%DS) were made when necessary.

To assess intra-observer agreement, measurements were made twice per acquisition technique, with an interval of at least one month.

To evaluate image quality, every coronary segment with a reference diameter  $\geq 1.5$  mm was assessed by the same two radiologists. The primary reader performed the scoring while the second reader observed in a separate session; whenever interpretations differed, the score was discussed, and a consensus was reached on a single final score. Image quality was graded on a 5-point scale (modified from Achenbach et al.): 4 = excellent (full confidence regarding presence/absence of luminal stenosis); 3 = good (high confidence); 2 = moderate (minor doubts); 1 = poor (some doubts); 0 = non-diagnostic (relevant doubts).<sup>20</sup> The same consensus procedure was applied to all 18 segments of the Society of Cardiovascular Computed Tomography (SCCT) coronary segmentation model.<sup>21</sup> Because a consensus approach was used, inter-observer variability metrics were not calculated.

### 2.5. Invasive coronary angiography with quantitative coronary analysis (ICA/QCA)

A cardiologist (C.P) with more than ten years of experience of ICA reading, performed the analysis of the ICA examinations. Whenever possible, two orthogonal views of the assessed stenotic segments were obtained, and a mean value of the observed QCA stenosis grade was computed. The analysis was performed using a dedicated workstation (AW 4.7, GE Healthcare, Chicago, IL, USA) with stenosis analysis (QCA) software version 1.6.

While referred patients had suspected stenoses based on CT, the reader of the CCTA images was blinded to the QCA measurements.

Whenever discrepancies were noted between the CCTA and ICA, the examinations were reviewed again together with a radiologist (G.W) with more than 20 years of experience of cardiac reading in both ICA and CCTA, to verify that identified coronary lesions were allocated to the same coronary segments in ICA and CCTA.

### 2.6. Statistical analysis

All statistical analyses were performed using IBM SPSS Statistics for Windows, version 29.0.2.0 (IBM Corp., Armonk, NY, USA) or Python 3.11. Continuous variables are presented as mean  $\pm$  standard deviation (SD) if normally distributed, or as median and range otherwise. Normality of distribution was assessed using the Shapiro–Wilk test.

Differences in radiation dose and contrast volume between EID-CT and PCD-CT were compared using paired Student's t-tests, assuming normal distribution.

Diagnostic accuracy of detecting significant stenosis was assessed on a per-segment basis ( $n = 301$  segments), accounting for within-patient clustering.<sup>22</sup> The reference standard was QCA derived from ICA, with a diameter stenosis  $\geq 50\ %$  considered hemodynamically significant. For each CT modality, receiver operating characteristic (ROC) curves were generated using the continuous %DS values against the binary QCA reference. The area under the ROC curve (AUC) and its 95 % confidence interval (CI) were estimated and compared with a patient-level

**Table 2**  
Subject characteristics (n = 21).

Patient Characteristics		
Sex (female, %)	5 (24 %)	
Age (years)	71.5 ± 2.1	
Body Mass index (BMI)	25.6 ± 1.0	
Diabetes (%)	3 (14 %)	
Hypertension (%)	18 (86 %)	
Active or former smoker (%)	11 (52 %)	
Lipid-lowering medication (%)	15 (71 %)	
Agatston Score Distribution		
Score Range	n (%)	
≥1000	7 (33.3 %)	
400–1000	5 (23.8 %)	
100–400	5 (23.8 %)	
<100	4 (19.0 %)	
CAD-RADS Categories by Modality		
CAD-RADS	EID-CT	PCD-CT
0–1	0	0
2	3	5
3	8	8
4	7	3
5	3	5

(clustered) bootstrap, resampling at the patient level to preserve intra-patient correlation.<sup>22</sup> Diagnostic performance metrics (sensitivity, specificity, accuracy, PPV, and NPV) were computed at a prespecified threshold of %DS ≥ 50 % on CT.

Lesions exhibiting >30 %DS in vessels with a diameter >1.5 mm were included to compare agreement across EID-CT, PCD-CT and QCA-derived %DS values. The agreement across all segments was assessed using Friedman tests and Bland–Altman analysis. Spearman's correlation coefficient ( $\rho$ ), as well as Bland–Altman analysis was used to assess intra-observer agreement.

Qualitative image quality was compared between PCD-CT and EID-CT using the Wilcoxon signed-rank test for paired ordinal data. Two comparisons were performed: one including all coronary segments (segments 1–18) and another on a per-segment basis. For the per-

segment analysis, p-values were adjusted for multiple comparisons using the Benjamini-Hochberg procedure to control the false discovery rate. A two-sided  $p < 0.05$  was considered statistically significant for the overall comparison, and a false discovery rate (FDR) < 0.05 was used to determine significance in the per-segment analysis.

### 3. Results

#### 3.1. Participant and clinical characteristics

A total of 21 participants were included in the study, of whom 5 were women and 16 were men. Clinical characteristics are summarized in Table 2. The mean interval between the two CT examinations was  $44 \pm 31$  days, and the mean interval between the initial CT and the ICA was  $63 \pm 34$  days. According to the Shapiro–Wilk test, the distributions of radiation dose differences and contrast agent dose differences were consistent with normality ( $p = 0.15$  and  $p = 0.11$ , respectively). Paired t-tests revealed that the radiation dose was significantly lower in PCD-CT compared to EID-CT ( $p < 0.01$ ). In addition, contrast volume was significantly lower in PCD-CT compared to EID-CT ( $p = 0.01$ ).

#### 3.2. Quantitative analysis of diameter stenosis (%DS)

A total of 301 coronary segments were analyzed on a per-segment basis. Among the detected plaques, five were purely non-calcified, while the remainder were either calcified or mixed. Example images of calcified coronary artery segments are shown in Fig. 1. On QCA, 39 segments demonstrated significant stenosis, whereas 37 and 39 segments were classified as having obstructive disease on EID-CT and PCD-CT, respectively. Lesions were predominantly located in proximal coronary segments (segments 1, 2, 5–9, and 11), affecting 80 % of patients. ROC analysis yielded a per-segment, cluster-corrected AUC of 0.86 (0.77–0.93) for EID-CT and 0.89 (0.83–0.94) for PCD-CT (Fig. 2). Diagnostic performance metrics were not significantly different between EID-CT and PCD-CT ( $p > 0.63$ ) and are presented in Table 3.

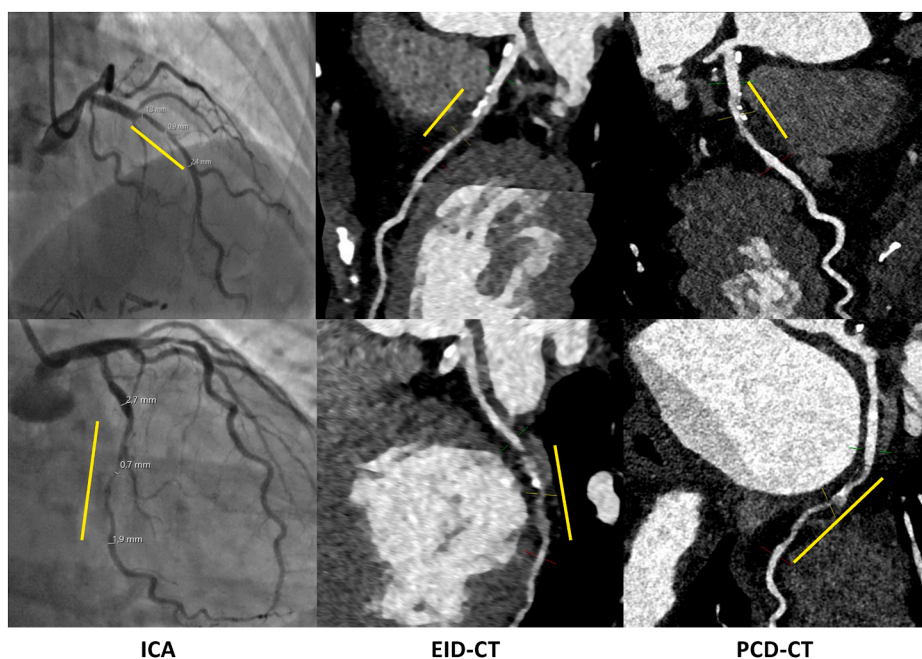


**Fig. 1.** Example of coronary stenosis assessment using invasive coronary angiography (ICA), energy-integrating detector CT (EID-CT), and photon-counting detector CT (PCD-CT). Calcified coronary artery segments with significant stenosis are shown in the proximal left anterior descending artery (LAD; top row) and the mid left circumflex artery (CX; bottom row). Images are displayed for ICA (left), coronary CT angiography acquired with EID-CT using a Bv36 kernel (middle), and PCD-CT using a Bv64 kernel (right). In segment 7, the measured percentage diameter stenosis (%DS) was 80 %, 49 %, and 53 % for ICA, EID-CT, and PCD-CT, respectively; corresponding values in segment 13 were 62 %, 64 %, and 64 %. Image quality scores were 2 (segment 7) and 0 (segment 13) for EID-CT, and 3 (segment 7) and 2 (segment 13) for PCD-CT. PCD-CT demonstrates improved lumen delineation and reduced blooming artifacts compared with EID-CT, potentially increasing diagnostic confidence in stenosis grading.

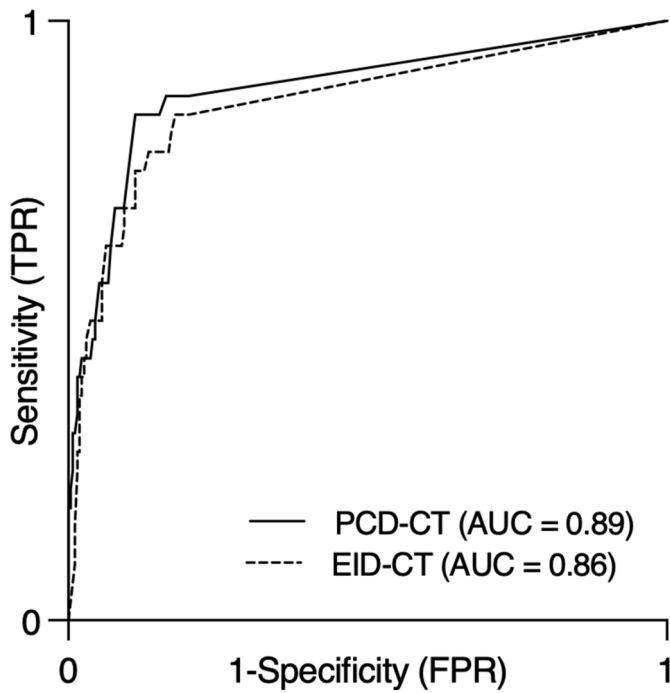


**Fig. 2.** Diagnostic performance of EID-CT and PCD-CT for detecting significant coronary artery stenosis. Receiver operating characteristic (ROC) curves illustrating the diagnostic accuracy of EID-CT and PCD-CT for detecting  $\geq 50\%$  coronary artery stenosis, at a segmental level, using ICA as the reference standard. Both modalities showed good diagnostic performance with similar area under the curve (AUC) values (EID-CT: 0.86; PCD-CT: 0.89), reflecting comparable overall accuracy in this participant cohort.

Across all coronary segments with available data, no statistically significant difference in %DS was found across QCA, EID-CT and PCD-CT ( $\chi^2 = 3.24$ ,  $p = 0.20$ ). When restricting the analysis to segments with measurable stenosis in all three modalities, no significant difference was observed either ( $\chi^2 = 0.61$ ,  $p = 0.74$ ). Bland-Altman analysis demonstrated close agreement between modalities. The mean difference in % DS was 1.2 % between QCA and EID-CT (limits of agreement: 37.3 % to +34.8 %) and 1.2 % between QCA and PCD-CT (-34.5 % to +32.0 %). Between EID-CT and PCD-CT, the mean difference was 0.0 % and limits of agreement ranged from -25.0 % to +24.9 % (Fig. 3).

**3.3. Intra-observer reproducibility of %DS measurements**

Intra-observer agreement was strong for both CT systems, with a Spearman's  $\rho = 0.91$  ( $p < 0.05$ ) for both EID-CT and PCD-CT. Bland-Altman analysis for repeated measurements showed a mean difference of 1.47 % (limits of agreement: 19.2 %–22.1 %) for EID-CT and a mean difference of 1.02 % (limits of agreement: 22.3 %–24.5 %) for PCD-CT.

**Table 3**  
Diagnostic Performance (per-segment analysis, n = 301 segments).

Metric	EID-CT (mean, 95 % CI)	PCD-CT (mean, 95 % CI)	p-value
Accuracy	0.90 (0.87–0.94)	0.90 (0.86–0.94)	0.77
Sensitivity	0.62 (0.50–0.75)	0.62 (0.48–0.76)	1.0
Specificity	0.94 (0.90–0.97)	0.93 (0.89–0.96)	0.63
Positive predictive value (PPV)	0.54 (0.37–0.71)	0.51 (0.35–0.66)	0.67
Negative predictive value (NPV)	0.95 (0.93–0.98)	0.95 (0.93–0.98)	0.96
True positive (TP)	22	23	
False positive (FP)	15	16	
True negative (TN)	247	246	
False negative (FN)	17	16	

**3.4. Image quality assessment**

Image quality scores were compared using the Wilcoxon signed-rank test, which revealed a significant difference between the two CT systems. In the analysis including all coronary segments, the mean image quality score was  $2.85 \pm 0.89$  for PCD-CT and  $2.49 \pm 0.84$  for EID-CT ( $p < 0.001$ ). A per-segment analysis showed that PCD-CT yielded higher median image quality scores than EID-CT in several segments. Statistically significant differences were observed in the right coronary artery, including the proximal (1), distal (3), and posterior descending (4) segments, as well as in the left main coronary artery (segment 7) ( $p < 0.04$ ), see Fig. 4.

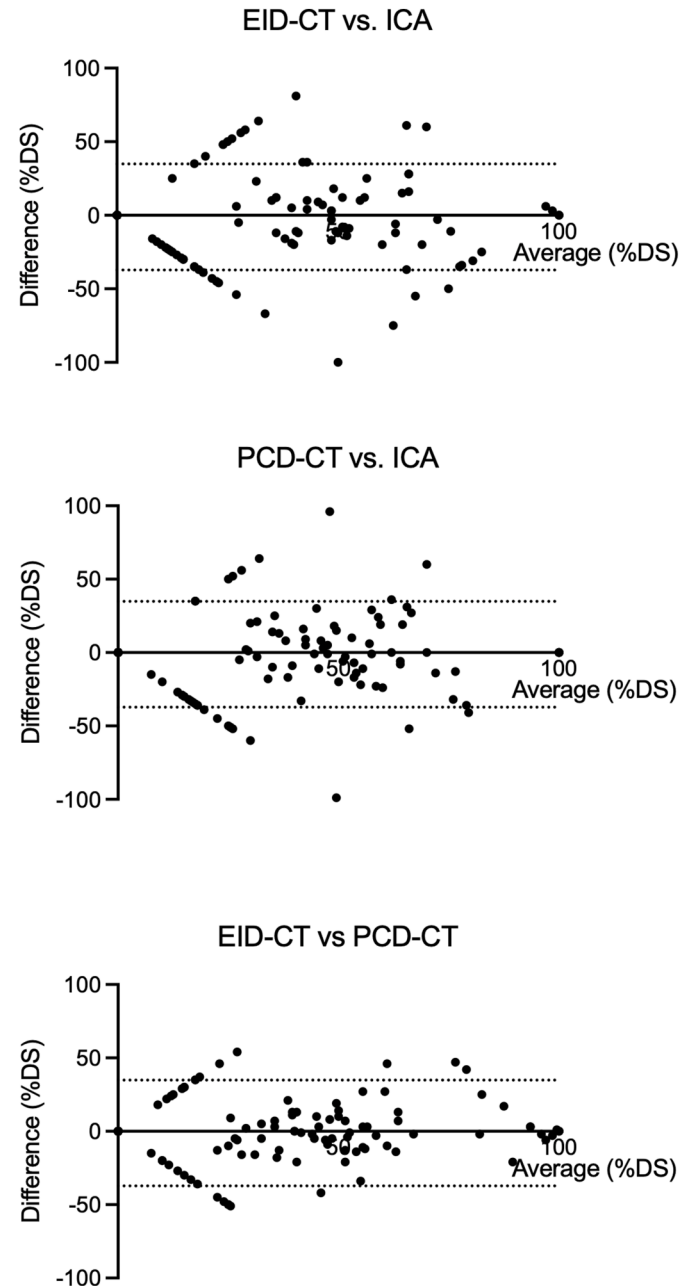


**Fig. 3.** Bland-Altman plots showing agreement in percentage diameter stenosis (%DS) between imaging modalities. Mean differences and 95 % limits of agreement ( $\pm 1.96$  SD) are shown for (a) QCA versus EID-CT, with a mean difference of 1.2 % (limits of agreement: 37.3 % to +34.8 %); (b) QCA versus PCD-CT, with a mean difference of 1.2 % (-34.5 % to +32.0 %); and (c) EID-CT versus PCD-CT, with a mean difference of 0.0 % (-25.0 % to +24.9 %).

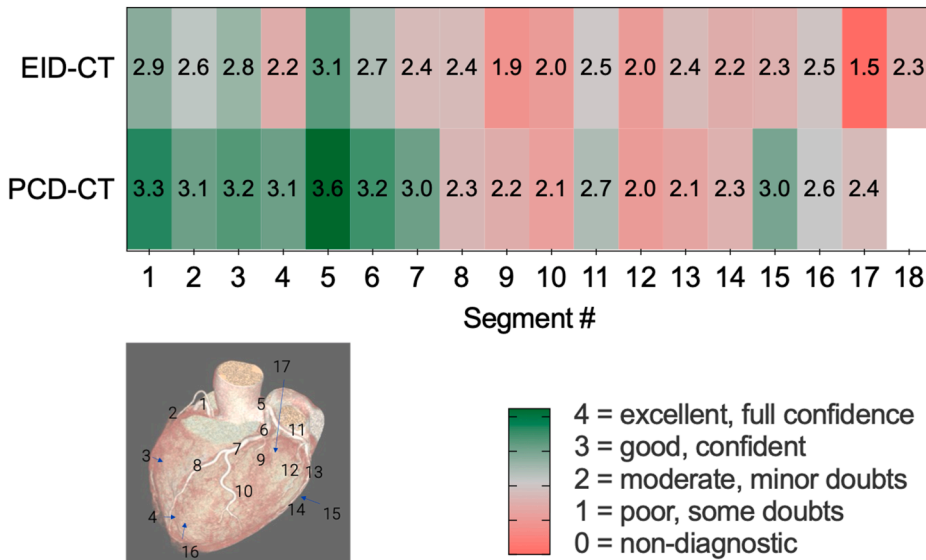


**Fig. 4. Distribution of image quality scores for PCD-CT and EID-CT.**

A per-segment analysis showed that PCD-CT yielded higher median image quality scores than EID-CT in several segments. Statistically significant differences were observed in the right coronary artery (RCA), including the proximal (segment 1), distal (3), and posterior descending (4) segments, as well as in the left main coronary artery (segment 7) ( $p < 0.04$ ).

Scores range from 0 to 4:

0 = non-diagnostic (relevant doubts about presence/absence of stenosis),  
 1 = poor quality (some doubts),  
 2 = moderate quality (minor doubts),  
 3 = good quality (confident),  
 4 = excellent quality (full confidence without any doubts).

#### 4. Discussion

In the currently available PCD-CT systems, the standard-resolution mode offers several practical advantages over UHR mode. The use of a larger detector width allows for shorter scan durations, which in the case of CCTA, reduces the risk for motion or stairstep artifacts, making the SR mode more robust in clinical routine. It is therefore often the preferred acquisition mode in patients with low calcium scores or highly irregular heart rates, as it minimizes the need for repeated scans.

The main finding in this study was that %DS values from PCD-CT, using standard-resolution mode, did not significantly differ from those of EID-CT, and that both showed good agreement with QCA. The mean radiation dose of the PCD-CT examinations was approximately 50 % lower than that of EID-CT. ROC analysis revealed good to high diagnostic performance, with high specificity and NPV, yet only moderate sensitivity and PPV were observed. PCD-CT was graded as having higher image quality than EID-CT.

Previous studies have reported partly different outcomes, often showing a diagnostic advantage of PCD-CT over EID-CT. Fahrni et al. compared EID-CT and PCD-CT (using UHR mode) with ICA and found improved diagnostic performance using PCD-CT.<sup>23</sup> Sakai et al. reported that participants examined with PCD-CT (using both SR and UHR mode) were less often referred for ICA, but more often underwent revascularization when ICA was performed. They also found improved specificity, PPV, and accuracy for PCD-CT, while sensitivity and NPV were similar to EID-CT.<sup>24</sup> Nakashima et al. showed that PCD-CT (using SR-as well as UHR-mode) significantly decreases the overestimation of stenosis and the misclassification of uncertain high-risk plaques, thereby reducing the frequency of unnecessary invasive angiography.<sup>25</sup>

There are also several studies comparing ICA and PCD-CT. Laux et al. demonstrated increased PPV when using UHR-PCD-CT.<sup>11</sup> Eberhard et al. found more accurate stenosis classification when using UHR mode compared to SR mode,<sup>10</sup> while Hagar et al. demonstrated good diagnostic accuracy in high-risk patients with Agatston scores  $\geq 1000$ .<sup>12</sup> Nishihara et al. showed that calcium-removal reconstructions improved specificity and PPV compared to standard reconstructions.<sup>26</sup> Vecsey-Nagy et al. compared PCD-CT in UHR mode with EID-CT, observing lower %DS values in PCD-CT and CAD-RADS reclassification in nearly half of cases.<sup>13</sup> In a study by Tremamunno et al., UHR PCD-CT showed fewer obstructive lesions and remodeling features but a more extensive CAD burden than EID-CT.<sup>27</sup> In contrast to our findings, Wolf et al. reported consistently lower %DS values with SR-PCD-CT than with EID-CT.<sup>28</sup>

Our results mostly align with these studies but also highlight some important aspects. The moderate sensitivity and PPV observed in our study may be explained by the use of SR rather than UHR mode in PCD-CT, as well as differences in acquisition protocols: EID-CT often used retrospective gating, improving evaluability but at the cost of higher radiation dose, while PCD-CT primarily used sequential gating. The lower radiation dose observed in PCD-CT is consistent with these protocol differences.

Another factor is the highly selected study population. Despite only 21 participants, 70 segments were truly diseased. Many had high Agatston scores (30 %  $\geq 1000$ ; 24 % between 400 and 999), most had CAD-RADS  $\geq 3$ , and 80 % showed significant ICA stenosis. Four underwent PCI and four were referred for CABG. These cases illustrate the diagnostic challenges of heavy calcification, which can reduce PPV and sensitivity. Nonetheless, image quality in PCD-CT was rated higher, consistent with findings from Sharma et al., who used UHR protocols.<sup>29</sup>

Another important finding is that, while PCD-CT consistently received higher image quality ratings than EID-CT in key segments, including the left main, LAD, and RCA, this did not lead to more accurate stenosis grading, likely due to the use of a SR-protocol. Unlike ultra-high-resolution modes, SR-PCD-CT lacks the spatial detail (e.g., 0.2 mm slices, sharper reconstruction kernels) needed to precisely assess small luminal changes, especially in heavily calcified or distal vessels.

This study has several strengths and limitations. A strength is that the study included participants who underwent repeated CCTA with both EID-CT and PCD-CT, as well as QCA. To our knowledge, few previous studies have compared stenosis measurements acquired in the same individuals using different CT systems, with QCA as the reference standard. However, limitations include the fact that EID-CT data were collected from three different scanners with six different tube voltage settings and a mix of high-pitch and retrospective gating. Also, PCD-CT protocols evolved during the study period, due to software updates and application of different kernel settings. The small and selected study population also limits generalizability. The %DS measurements and image quality scores were assigned through consensus between two experienced radiologists at the second reading session, which precluded calculation of inter-observer agreement. Finally, numerical stenosis measurements on CCTA are known to vary between readers and software solutions and are therefore not routinely recommended in current guidelines. Although measurements in this study were performed by experienced readers using a consensus approach, this represents an idealized research setting and may limit generalizability to everyday clinical practice.

In conclusion, SR-PCD-CT and EID-CT demonstrated comparable diagnostic accuracy for coronary artery stenosis grading, with good agreement to QCA. PCD-CT provided superior image quality and significantly lower radiation dose than EID-CT. However, both systems showed only moderate PPV particularly in cases with extensive coronary calcifications. These results, together with previous studies, suggest that while standard resolution PCD-CT offers a robust scan protocol and improved image quality compared with EID-CT, the use of UHR acquisition is required to improve stenosis evaluation, particularly in patients with high calcium burden.

### Informed consent

Written informed consent was obtained from all subjects (patients) in this study.

### Guarantor

The scientific guarantor of this publication is Anders Persson.

### Statistics and biometry

One of the authors has significant statistical expertise.

### Ethical approval

Institutional Review Board approval was obtained.

The study was approved by the Swedish Ethical Review Authority (Dnr 2022-04666-01) and performed in accordance with the Declaration of Helsinki. Written informed consent was obtained from all study participants.

### Study subjects or cohorts overlap

No subjects or cohort overlap.

### Methodology

#### Methodology.

- prospective
- observational
- performed at one institution

### Funding

The authors state that this research did not receive any specific grant from funding agencies in the public, commercial, or not-for-profit sectors.

### Declaration of competing interest

The authors of this manuscript declare no relationships with any companies, whose products or services may be related to the subject matter of the article.

### Acknowledgements

The authors are grateful to Gunnar Wiklund, MD, Linköping university hospital, Linköping, Sweden, for help with assessment of CCTA and ICA examinations.

### References

1. Sanchis-Gomar F, Perez-Quilis C, Leischik R, Lucia A. Epidemiology of coronary heart disease and acute coronary syndrome. *Ann Transl Med.* 2016;4:1–12. <https://doi.org/10.21037/atm.2016.06.33>.

2. Vrints C, Andreotti F, Koskinas KC, et al. ESC scientific document group. 2024 ESC guidelines for the management of chronic coronary syndromes. *Eur Heart J.* 2024; 45:1–123. <https://doi.org/10.1093/eurheartj/ehae177>.
3. Barrett HE, van der Heiden K, Farrell E, Gijsen FJH, Akyildiz AC. Calcifications in atherosclerotic plaques and impact on plaque biomechanics. *J Biomech.* 2019;87: 1–12. <https://doi.org/10.1016/j.jbiomech.2019.03.005>.
4. Narula J, Chandrashekar Y, Ahmadi A, et al. SCCT 2021 expert consensus document on coronary computed tomographic angiography. *J Cardiovasc Comput Tomogr.* 2021;15:192–217. <https://doi.org/10.1016/j.jcct.2020.11.001>.
5. Cury RC, Leipsic J, Abbara S, et al. CAD-RADS™ 2.0—2022 coronary artery disease—reporting and data system. *J Cardiovasc Comput Tomogr.* 2022;16:536–557. <https://doi.org/10.1016/j.jcct.2022.07.002>.
6. Nieman K, García-García HM, Hideo-Kajita A, et al. Standards for quantitative assessments by coronary computed tomography angiography. *J Cardiovasc Comput Tomogr.* 2024;18:429–443. <https://doi.org/10.1016/j.jcct.2024.05.232>.
7. Flohr T, Ulzheimer S, Petersilka M, Schmidt B. Basic principles and clinical potential of photon-counting detector CT. *Chin J Acad Radiol.* 2020;3:19–34. <https://doi.org/10.1007/s42058-020-00029-z>.
8. Willeminck MJ, Persson M, Pourmorteza A, Pelc NJ, Fleischmann D. Photon-counting CT: technical principles and clinical prospects. *Radiology.* 2018;289:293–312. <https://doi.org/10.1148/radiol.2018172656>.
9. Leng S, Bruesewitz M, Tao S, et al. Photon-counting detector CT: system design and clinical applications of an emerging technology. *Radiographics.* 2019;39:729–743. <https://doi.org/10.1148/rg.2019180115>.
10. Eberhard M, Candreva A, Rajagopal R, et al. Coronary stenosis quantification with ultra-high-resolution photon-counting detector CT angiography. *JACC: Cardiovasc Imaging.* 2024;17:342–344. <https://doi.org/10.1016/j.jcimg.2023.10.004>.
11. Laux GS, Halfmann MC, Kavermann L, et al. Ultra-high-resolution photon-counting detector coronary CT minimizes overestimation bias compared with invasive reference. *Eur J Radiol.* 2025;188:112154. <https://doi.org/10.1016/j.ejrad.2025.112154>.
12. Hagar MT, Soschynski M, Saffar R, et al. Accuracy of ultra-high-resolution photon-counting CT for detecting coronary artery disease in a high-risk population. *Radiology.* 2023;307:1–10. <https://doi.org/10.1148/radiol.223305>.
13. Vecseynagy M, Tremamunno G, Schoepf UJ, Gnasso C. Intraindividual comparison of ultra-high-spatial-resolution photon-counting detector CT and energy-integrating detector CT for coronary stenosis measurement. *Circ: Cardiovasc Imaging.* 2024;17: e017112. <https://doi.org/10.1161/CIRCIMAGING.124.017112>.
14. Bolognese L, Reccia MR. Computed tomography to replace invasive coronary angiography? The DISCHARGE trial. *Eur Heart J Suppl.* 2022;24:125–128. <https://doi.org/10.1093/eurheartjsupp/suac067>.
15. Lim MJ, White CJ. Coronary angiography is the gold standard for patients with significant left ventricular dysfunction. *Prog Cardiovasc Dis.* 2013;55:504–508. <https://doi.org/10.1016/j.pcad.2013.01.003>.
16. Campeau L. Grading of angina pectoris. *Circulation.* 1976;54:522–523. <https://doi.org/10.1161/01.CIR.54.3.522>.
17. Dagenais GR, Armstrong PW, Thérioux P, Naylor CD. Revisiting the Canadian cardiovascular society grading of stable angina pectoris. *Can J Cardiol.* 2002;18: 941–944.
18. Knuuti J, Wijns W, Saraste A, et al. ESC scientific document group. 2019 ESC guidelines for the diagnosis and management of chronic coronary syndromes. *Eur Heart J.* 2020;41:407–477. <https://doi.org/10.1093/eurheartj/ehz425>.
19. Diamond GA, Forrester JS. Analysis of probability as an aid in the clinical diagnosis of coronary-artery disease. *N Engl J Med.* 1979;300:1350–1358. <https://doi.org/10.1056/NEJM197906143002402>.
20. Achenbach S, Paul JF, Laurent F, et al. Comparative assessment of image quality for coronary CT angiography with different iodine concentrations. *Eur Radiol.* 2017;27: 821–830. <https://doi.org/10.1007/s00330-016-4437-9>.
21. Leipsic J, Abbara S, Achenbach S, et al. SCCT guidelines for the interpretation and reporting of coronary CT angiography. *J Cardiovasc Comput Tomogr.* 2014;8: 342–358. <https://doi.org/10.1016/j.jcct.2014.07.003>.
22. Rutter CM. Bootstrap estimation of diagnostic accuracy with patient-clustered data. *Acad Radiol.* 2000;7:413–419. [https://doi.org/10.1016/S1076-6332\(00\)80381-5](https://doi.org/10.1016/S1076-6332(00)80381-5).
23. Fahmi G, Boccalini S, Mahmoudi A, et al. Quantification of coronary artery stenosis in very-high-risk patients using ultra-high-resolution spectral photon-counting CT. *Investig Radiol.* 2024;59:1–9. <https://doi.org/10.1097/RLI.0000000000001109>.
24. Sakai K, Shin D, Singh M, et al. Diagnostic performance and clinical impact of photon-counting detector CT in coronary artery disease. *J Am Coll Cardiol.* 2024;85: 1–12. <https://doi.org/10.1016/j.jacc.2024.10.069>.
25. Nakashima M, Miyoshi T, Hara S, et al. Photon-counting CT enhances diagnostic accuracy in stable coronary artery disease. *J Clin Med.* 2025;14:6049. <https://doi.org/10.3390/jcm14176049>.
26. Nishihara T, Miyoshi T, Nakashima M, et al. Diagnostic improvements of calcium-removal image reconstruction using photon-counting detector CT. *Eur J Radiol.* 2024;172:111354. <https://doi.org/10.1016/j.ejrad.2024.111354>.
27. Tremamunno G, Varga-Szemes A, Schoepf UJ, et al. Semiquantitative metrics of coronary artery disease burden. *J Cardiovasc Comput Tomogr.* 2025;19:474–482. <https://doi.org/10.1016/j.jcct.2025.04.012>.
28. Wolf EV, Gnasso C, Schoepf UJ, et al. Intraindividual comparison of coronary artery stenosis measurements between energy-integrating detector CT and photon-counting detector CT. *Imaging.* 2023;15:4–11. <https://doi.org/10.1556/1647.2023.00156>.
29. Sharma SP, Budde RPJ, Groen JW, et al. Comparison of image quality between photon-counting detector CT and energy-integrating detector coronary CT angiography in heart transplant patients. *Int J Cardiovasc Imag.* 2025;41:1–10. <https://doi.org/10.1007/s10554-025-03433-7>.